Journal of Medical Microbiology (2013), **62**, 69–77 DOI 10.1099/jmm.0.047811-0

Synergistic bactericidal activity between hyperosmotic stress and membrane-disrupting nanoemulsions

Sean Connell,[1] Jianming Li[2] and Riyi Shi[1,2]

[1]Weldon School of Biomedical Engineering, Purdue University, West Lafayette, IN 47907, USA

[2]Department of Basic Medical Sciences, Purdue University, West Lafayette, IN 47907, USA

Correspondence
Jianming Li
Riyi Shi
Jianming@purdue.edu

There is a clear clinical need for alternative types of non-antibiotic biocides due to the rising global health concern of microbial drug resistance. In this work, a novel antibacterial concept was delineated that utilized hyperosmotic stress (H) in concert with membrane-disrupting nanoemulsions (NEs). The antibacterial effects of either H or a NE, as well as in combination (H+NE), were assessed *in vitro* using an *Escherichia coli* model. It was found that exposure to H or NE alone produced dose-dependent bacteriostatic and bactericidal effects, respectively. However, the bactericidal action of NE was significantly amplified in the presence of H. Outcomes following H+NE exposure included rapid efflux of K^+ and nucleic acids, increased membrane permeability and a reduction in both intracellular ATP and cell viability. Further inspection of morphology by electron microscopy highlighted cell shrinkage, membrane dissolution and bacteriolysis. Pathogen inactivation occurred immediately upon contact with H+NE. The effects of H, NE and H+NE against *Enterococcus faecalis*, *Staphylococcus aureus* and meticillin-resistant *S. aureus* isolates were also examined. Similar to the *Escherichia coli* model, H+NE showed antibacterial synergism in these organisms when classified by the Chou–Talalay combination index for two-agent interactions. This synergistic interaction suggests that the H+NE platform may potentially serve as a new paradigm in disinfectants, antiseptics and antibacterial wound dressings. The H+NE mechanism of action was termed osmopermeation, as a descriptor for the underlying inactivation process.

Received 29 May 2012
Accepted 25 September 2012

INTRODUCTION

The impetus for investigating new non-antibiotic biocides is evident. In the past 20 years, the Centers for Disease Control and Prevention have estimated that the rate of drug resistance has increased by 36 %. This trend is exacerbated by limitations in drug discovery. In fact, no new structural classes of antibiotics have been developed since 1963 (Hancock, 2007). These statistics highlight the necessity of developing original antimicrobial approaches with wide-spectrum properties.

One well-established strategy for inhibiting bacterial proliferation is the use of hyperosmotic stress (H) treatment generated by non-ionic saccharides or polyols. These non-ionic hyperosmotic solutes possess relatively low toxicity and have been exploited in food preservation and in the clinical setting (Gould, 1996; Middleton & Seal, 1990; O'Byrne & Booth, 2002). At the cell level, H treatment has been shown to cause cell shrinkage, upregulate starvation genes, decrease DNA replication and inhibit proliferation (Csonka, 1989; Csonka & Hanson, 1991; Pilizota & Shaevitz, 2012; Wood, 2011). However, the effects of H can be mitigated by adaptive cellular mechanisms (Wood, 1999), including the synthesis of compatible solutes and a reduction in cell volume (Brill *et al.*, 2011; Christian & Waltho, 1961; Pilizota & Shaevitz, 2012; Wood, 2011). Through these osmoregulatory processes, strains such as *Staphylococcus aureus* can withstand osmotic pressures near 10 MPa, which is estimated to be the threshold for cell-wall failure (Carpita, 1985). Bacterial viability at such extreme conditions makes practical implementation of hyperosmotic gradients difficult, as it requires saccharide concentrations near solubility limits.

In this work, our goal was to investigate the interaction effects between H and membrane disruption as a potential tool for bacterial remediation. Our rationale for combining membrane disruption with a hypertonic environment originated from cell biomechanics. As the intact cell membrane plays a key role in regulating osmotic equilibrium, we postulated that disrupting cell permeability would

Abbreviations: BCl, benzethonium chloride; CI, combination index; H, hyperosmotic stress; MRSA, meticillin-resistant *Staphylococcus aureus*; NE, nanoemulsion; PI, propidium iodide; SEM, scanning electron microscopy; TEM, transmission electron microscopy.

compromise the cell's capacity to accommodate mild osmotic shifts and ultimately induce cell death. This technique, which we call osmopermeation, exploits fundamental cell-membrane biophysics. Osmopermeation was conceived as a means of developing antibacterials with low *in vivo* toxicity and to enhance the application scope of hyperosmotic agents. Sucrose was used as the non-ionic osmoticum to induce H, whilst thymol-based nanoemulsions (NEs) were used to increase membrane permeability. These compounds were selected initially for proof of concept because of their well-known mechanisms of action and historical context in medicine.

In this study, we have illustrated the mechanism and kinetics of H, NE and their combined use (H + NE) using a pathogenic *Escherichia coli* model. Direct and indirect markers for cell damage were used in conjunction with electron microscopy to assess changes in cell viability and morphology. The antibacterial effects of H + NE were also tested on Gram-positive *Enterococcus faecalis*, *S. aureus* and meticillin-resistant strains of *S. aureus* (MRSA). The experimental results provide a conceptual framework for a new bactericidal strategy suitable for further *in vivo* testing.

METHODS

Bacterial strains and culture conditions. *Escherichia coli* ATCC 8739, *S. aureus* ATCC 6538, MRSA ATCC 43300 and *Enterococcus faecalis* ATCC 29212 were obtained from the American Type Culture Collection and cultured using Mueller–Hinton II cation-adjusted broth (pH 7.0). The inoculation densities for each method as described below were determined optically using a Perkin Elmer Lambda 25 spectrophotometer at 600 nm. Unless noted, bacterial suspensions were diluted to a McFarland standard no. 1.0 and aliquots were removed to achieve the desired concentration in the medium. For all experiments, bacteria were incubated at 37 °C in the appropriate treatment. Sucrose was used to generate osmotic conditions of 0.29–2.92 M (0.7–7.4 MPa). Osmotic pressures were calculated using the Van 't Hoff equation.

Synthesis and characterization of NEs. Membrane permeabilization was achieved with 2-isopropyl-5-methylphenol (thymol)-based emulsions, ranging in concentration from 0.33 to 6.6 mM (Walsh *et al.*, 2003). The thymol-based emulsions were produced by sonication techniques common to emulsion formation. The mean emulsion diameter was 184.3 nm with a polydispersity index of 0.180, as determined in eight sample runs using dynamic light scattering (Zetasizer; Malvern Instruments). Reagent-grade sucrose (>99.5 %) and thymol (>99.5 %) were purchased from Sigma Aldrich. H + NE was achieved by combining H with the membrane-permeabilizing NE at specified concentrations. Several initial tests at different hyperosmolarities and thymol concentrations were run to gauge the MICs. After these trials, selected combinations were used for subsequent experimentation. Studies were conducted in triplicate and repeated at least twice.

Cell-membrane integrity. For cell-membrane studies, *Escherichia coli* diluted to ~1.0×10^9 c.f.u. ml^{-1} was exposed to isotonic PBS (negative control), osmotic stress (1.17 M), NE disruption (2.66 mM), H + NE (1.17 M + 2.66 mM) and 0.01 % benzethonium chloride (BCl; positive control). After 1 h of exposure, the bacteria were isolated by centrifugation at 12 000 ***g*** for 10 min. The medium was decanted and the cell pellet resuspended in 5 ml PBS. Propidium iodide (PI; 25 µl at a final concentration of 5 µg ml^{-1}) was then placed in each sample and the cells were incubated for an additional 30 min in the dark at room temperature. Following staining, the bacteria were centrifuged, washed and resuspended in 1 ml PBS. Sample fluorescence was read using a Cytofluor 4000 (Applied Biosystems) with 488/570 nm excitation and emission filters. Background fluorescence was subtracted from all samples. For microscopy, PI-stained cells were prepared by pipetting 15 µl stained cells onto a coverslip. Photographs were imaged with a Nikon Diaphot 200 fluorescence scope and a CCD sensor (Diagnostic Instruments). Images in bright-field (threshold using ImageJ; NIH) and fluorescence modes were used to qualitatively show the number of stained bacteria.

Measurement of K^+. The degree of membrane damage was estimated by measuring the leakage of intracellular constituents, including K^+ and nucleic acids (Codling *et al.*, 2003; Walsh *et al.*, 2003). Potassium leakage was monitored with an ion-selective probe (6230M Metre; Jenco Instruments). *Escherichia coli* suspensions adjusted to a final concentration of 1.0×10^9 c.f.u. ml^{-1} in PBS were again subjected to 1.17 M osmotic stress, 2.66 mM NE, 1.17 M + 2.66 mM of the combination and 0.01 % BCl. Potassium leakage was monitored over a 1 h period with measurements recorded every 5 s using a 0.5 ml sample. The total available intracellular K^+ pool was estimated by boiling an untreated suspension of 1.0×10^9 c.f.u. bacteria ml^{-1} for 30 min. Sterile PBS served as a blank. Values are reported as the percentage of the total K^+ pool obtained from boiling.

Loss of 260 nm-absorbing material. Cytosolic leakage of nucleic acids was determined by measuring the amount of 260 nm-absorbing material (Chen & Cooper, 2002). *Escherichia coli* cultures were adjusted to a final cell suspension of 1.0×10^9 c.f.u. ml^{-1} and incubated for 1 h under the same treatment conditions outlined in the K^+ leakage experiments. The suspension was centrifuged for 10 min at 12 000 ***g*** and the resulting lysate was filtered twice using 0.22 µm filters to remove any remaining planktonic bacteria. The absorbance at 260 nm of the filtered lysate was recorded using a Perkin Elmer Lambda 25 spectrophotometer. Total cytosolic nucleic acid content was estimated by boiling an untreated suspension of bacteria for 30 min. Sterile PBS served as a blank.

Metabolic activity and c.f.u. enumeration. Intracellular ATP content was measured using an ATP-coupled luminescence assay (BacTiterGlo; Promega). *Escherichia coli* at a density of ~1.0×10^9 c.f.u. ml^{-1} was exposed to 1.17 M osmotic stress, 2.66 mM NE, 1.17 M + 2.66 mM of the combination and 0.01 % BCl for up to 1 h. Next, 100 µl of the *Escherichia coli* solutions was placed in a 96-well immunoassay plate. Intracellular ATP was extracted following protocols recommended by the assay manufacturer. Luminescence was measured with a Dynex MLX Microplate Luminometer (Magellan Biosciences). Samples were normalized to the background luminescence. Colony counting was performed using traditional agar-plating techniques. *Escherichia coli* grown to ~1.0×10^8 c.f.u. ml^{-1} was exposed to the designated treatments as outlined in the ATP assay. At time points of 10 min and 1 h, 200 µl of the sample fluid was removed, diluted up to 1 : 10 000 and streaked onto agar plates. At 24 h after plating, the dishes were scanned using a Microtek Scanmaker i800 flatbed scanner and the number of c.f.u. tabulated using ImageJ software.

Electron microscopy. *Escherichia coli* exposed to 1 h of H, NE and H + NE treatments were prepared using standard methods for electron microscopy imaging. For scanning electron microscopy (SEM), cells were fixed with a buffer solution of 2 % paraformaldehyde, 2.5 % glutaraldehyde and 0.1 M cacodylate for 8 h. Samples were then filtered through a 0.2 µm nucleopore membrane and further prepared using critical-point drying. Specimens were

mounted onto metal discs and sputter-coated with platinum. Images were taken with a FEI NOVA nanoSEM field emission scanning electron microscope using a 5 kV accelerating voltage. For transmission electron microscopy (TEM) imaging, bacteria were fixed as above for 1 h using the microwave method and with a secondary treatment of OsO_4. Cells were dispersed in 1.5 % agarose, spun down into a pellet and serially dehydrated with ethanol. Cells were then embedded and sectioned for imaging on an FEI/Philips CM-10 transmission electron microscope. An acceleration voltage of 80 kV was used.

Dose–response curves and determination of interaction. Dose–response curves of each bacterial strain to osmotic stress and membrane-permeabilizing NEs were generated using broth microdilution methods. Briefly, 5 ml medium was inoculated with each bacterial strain at a density of $\sim 1.0 \times 10^6$ c.f.u. ml^{-1}. After 24 h incubation with treatment, 300 µl medium was pipetted into a 96-well plate and the optical density (OD) was read at 620 nm using a Biochrom Asys 96 plate reader set. The OD_{620} for H, NE and H + NE treatments was recorded using CompuSyn software. Dose–response curves were generated automatically. The MIC for each treatment was determined using 95 % transparency as the clarity cut-off. Additionally, the combination index (CI) for specific combinations of H and NE was calculated using the Chou–Talalay method (Chou, 2006). Isobolograms plotted for each bacterial strain were tested using CompuSyn software.

Statistical methods. All data are means ± SEM. Statistical analysis was conducted using Student's *t*-test or one-way analysis of variance. The Tukey test was used for post-hoc evaluation. In all cases, a value of $P<0.05$ was considered significant.

RESULTS

Cell-membrane integrity

Representative fluorescent PI images and their bright-field counterparts for each treatment for *Escherichia coli* and the total fluorescence intensities are illustrated in Fig. 1(a, b). BCl (0.01 %) was used as the positive control. H treatment produced an insubstantial but significant increase in PI staining after 1 h incubation, with a fluorescence intensity of 76.67 ± 0.33 AU ($P<0.001$). Conversely, PI uptake increased in the NE-treated group, with a total fluorescence of 215.33 ± 1.20 AU ($P<0.001$). Cells treated with the H + NE combination demonstrated the greatest amount of PI staining (877.33 ± 6.0 AU) and were comparable to the values obtained for 0.01 % BCl (640 ± 8.7 AU).

K^+ leakage

Leakage of cytosolic content is indicative of the loss of function of membrane integrity. Changes in intracellular K^+ were monitored using an ion-selective probe (Fig. 1c, graph truncated to 30 min) for 1 h. H treatment resulted in a net influx of K^+ (7.1 ± 2.0 %) after 30 min of exposure and reached a steady state. Conversely, disruption of the cellular membrane with NE resulted in rapid efflux of K^+ in the first few minutes, reaching a maximum value of 15.0 ± 6.75 % ($P<0.001$) after 30 min of exposure

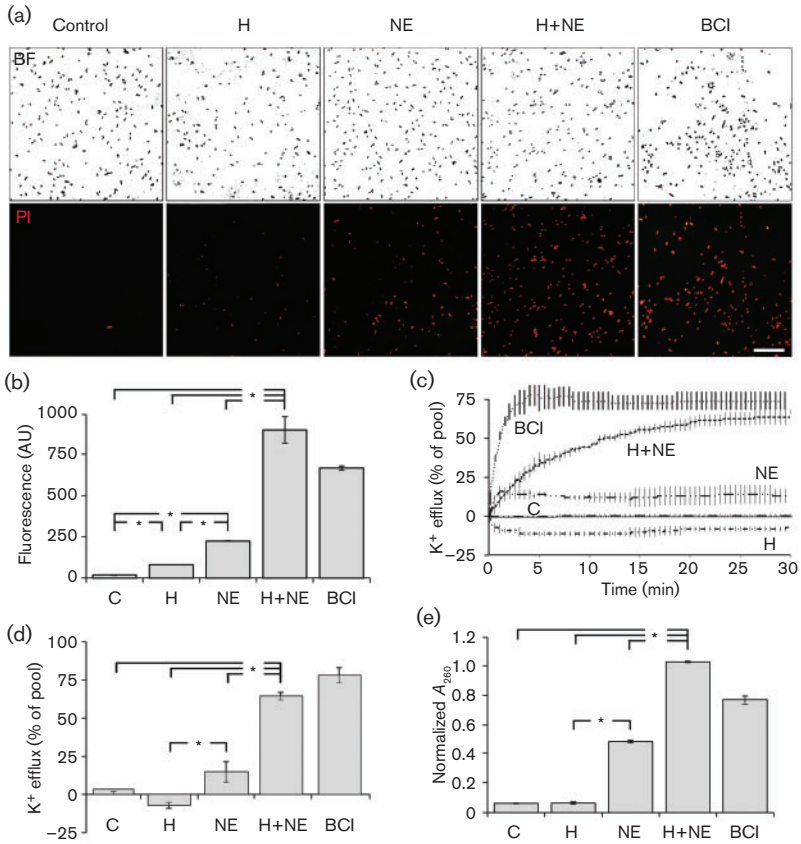

Fig. 1. (a) Bright-field (BF) images (top row) depicting *Escherichia coli* cells and corresponding PI images (bottom row) as a function of treatment regime (1 h). Concentrations of H, NE and the combination H + NE were 1.17 M, 2.66 mM and 1.17 M + 2.66 mM, respectively. BCl (0.01 %) served as the positive control. Bar, 30 µm. (b) Total PI fluorescence readings for the different groups. All groups were statistically significant compared with the negative control and with each other. BCl (0.01 %) was used as a positive control for comparative display only. (c) Real-time extracellular K^+ fluctuations following treatment exposure. Positive values denote an increase in extracellular K^+ and negative values indicate a decrease. The graph was truncated to 30 min. (d) Steady-state K^+ quantification at 30 min post-treatment. (e) Normalized A_{260} readings of cell-culture lysate after 1 h of challenge. All normalized values are with respect to the same bacterial populations boiled for 30 min. *$P<0.001$. Data are means ± SEM.

(Fig. 1d). Treatment with H+NE resulted in a steady release of K^+ in the first 10 min, peaking at 64.5±2.5 % of the total K^+ pool ($P<0.001$). Untreated controls did not demonstrate a significant K^+ efflux, whilst 0.01 % BCl produced 77.8±6.4 % K^+ loss.

Leakage of 260 nm-absorbing material

Leakage of nucleic acids was estimated by measuring the amount of 260 nm-absorbing material present after 1 h of treatment (Fig. 1e) and normalized to the amount of leaked nucleic acids from boiled bacteria. Loss of intracellular material was not induced by hypertonic treatment (0.066±0.002). NE exposure slightly increased A_{260} to 0.517±0.009 ($P<0.001$). However, H+NE treatment substantially facilitated leakage after 1 h, resulting in an absorbance value of 1.049±0.005 ($P<0.001$). Finally, 0.01 % BCl produced a normalized leakage reading of 0.78±0.003.

Metabolic activity and cell viability

Metabolic activity showed that ATP production was slightly higher in the hypertonic medium and was reduced with the NE after 1 h of treatment (Fig. 2a). Cells exposed to H treatment showed a 39.7±1.4 % (10 min) and 30.7±1.6 % (1 h) increase in metabolic activity when compared with $t=0$ min. NE-treated cells showed a 63.8±0.8 % (10 min) and 71.1±0.6 % (1 h) loss in overall metabolic function. H+NE treatment significantly enhanced de-energization, with a 77.0±0.1 % (10 min) and 81.8±0.5 % (1 h) reduction in ATP production. For comparison, 0.01 % BCl served as a positive control with a 55.4±0.8 % (10 min) and 91.7±1.0 % (1 h) reduction in metabolic activity. Following ATP measurements, the remaining samples were plated onto agar dishes and incubated for 24 h to validate overall viability. Colony counting showed that H treatment had no substantial effect on the number of viable cells for the 1 h treatment time. Scans of the viable colonies are shown in Fig. 2(b). Cultures exposed to NE demonstrated a ~6 log reduction, whilst H+NE treatment resulted in a >8 log reduction (complete bactericidal action) after only 10 min. The positive control of 0.01 % BCl had a similar log decrease after only 10 min.

Cell morphology

TEM images of untreated *Escherichia coli* revealed common identifiable features such as a centralized nucleoid, ribosomal staining and periplasm (Fig. 3a). In contrast, exposure to H treatment at 1.17 M caused dispersal of the nucleoid and a significant reduction in the periplasmic space (Fig. 3b). The membrane was also wavy in appearance. *Escherichia coli* subjected to 6.6 mM NE showed less-dense ribosomal regions and signs of bacteriolysis (Fig. 3c). The periplasm was still clearly visible. However, there were numerous submicron vesicle-like attachments on the bacterial membrane. These vesicles possessed a dark-staining membrane layer and are hypothesized to be the emulsified bacterial membrane.

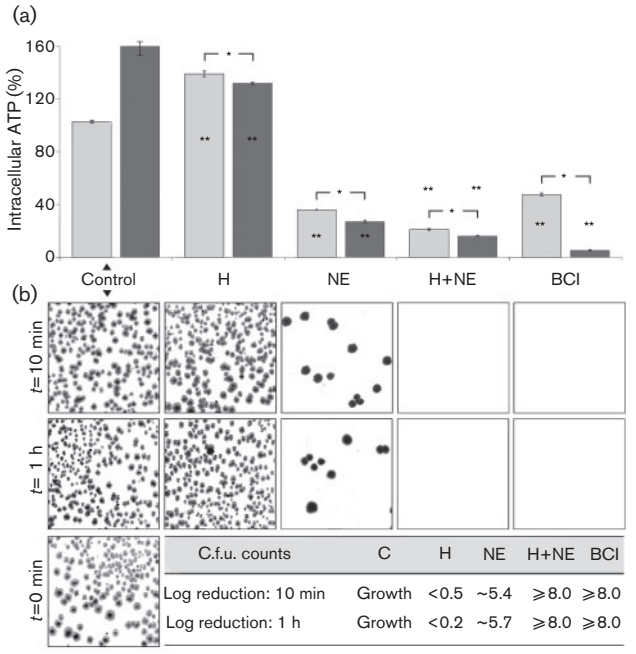

Fig. 2. (a) Intracellular ATP measurement in *Escherichia coli* cells after treatment times of 10 min and 1 h. Applied osmotic stress (H) was 1.17 M, whilst the NE concentration was 2.66 mM. The H+NE combination was 1.17 M+2.66 mM. Measurements were normalized to $t=0$ min ATP levels. All treatment groups were statistically significant compared with the untreated group and with all other treatments at their respective time points. ATP values were also significant when comparing 10 min and 1 h pairs for each treatment. Light grey bars, 10 min; dark grey bars, 1 h. *$P<0.001$; **$P<0.05$. Data are means±SEM. (b) Bacteria treated for 10 min and 1 h were further plated onto agar dishes for viability assessment. Corresponding plates (1 : 10 000 dilution for control untreated and H-treated dishes; 1 : 50 dilution for all others) after 24 h incubation are shown. The c.f.u. counts were consistent with the ATP trends, with the log decrease tabulated for each treatment condition.

Cells subjected to H+NE treatment demonstrated morphological features of both osmotic dehydration and membrane permeabilization (Fig. 3d, e). Exposed cells had a rougher surface texture, reduced periplasmic spacing and lighter intracellular staining (Fig. 4a–c). Denuded areas of membrane were also found and generally co-localized with membrane vesicles. These emulsion particles varied from <100 to 400 nm when analysed by SEM, and 77 % of all imaged H+NE-treated cells possessed some type of membrane bleb (Fig. 4e). Finally, a small number of treated cells exhibited lysis (4 %), as demonstrated by large cellular fragments and debris fields (Fig. 4e). Morphologically, the treated cells were significantly shorter than the controls. The length/diameter (L/D) ratio for treated bacteria was

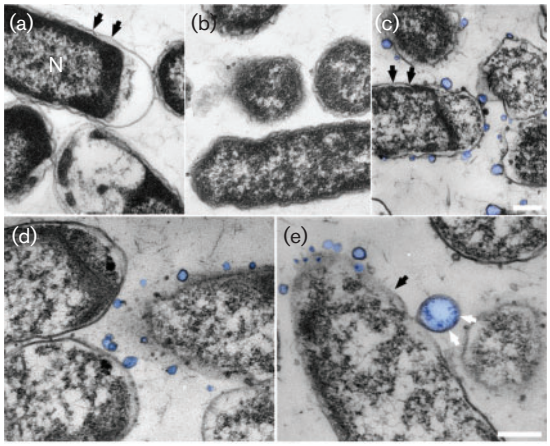

Fig. 3. (a) TEM images of untreated *Escherichia coli* cells. Black arrows highlight the periplasmic space, whilst N denotes the nucleoid. (b) TEM images of *Escherichia coli* subjected to H treatment (1.17 M) showing a shrunken morphology, a dispersed nucleoid and thinning of the periplasm. (c) TEM images of NE-treated (6.6 mM) cells. Black arrows depict the periplasm. Bacteriolysis is evident by the reduction in cytoplasmic staining. Numerous membrane-bound vesicles (pseudo-coloured in blue) were also observed attached to the outer membrane. (d, e) TEM images of *Escherichia coli* cells subjected to H+NE treatment (1.17 M+6.6 mM), showing disrupted cellular membranes and cell lysis. Again, membrane-bound vesicles were observed and are pseudo-coloured in blue. The black arrow in (e) demarcates an area of denuded membrane, whilst the white arrows indicate supposed ribosomal inclusions within the vesicle. Bars, 250 nm (a–c); 200 nm (d, e).

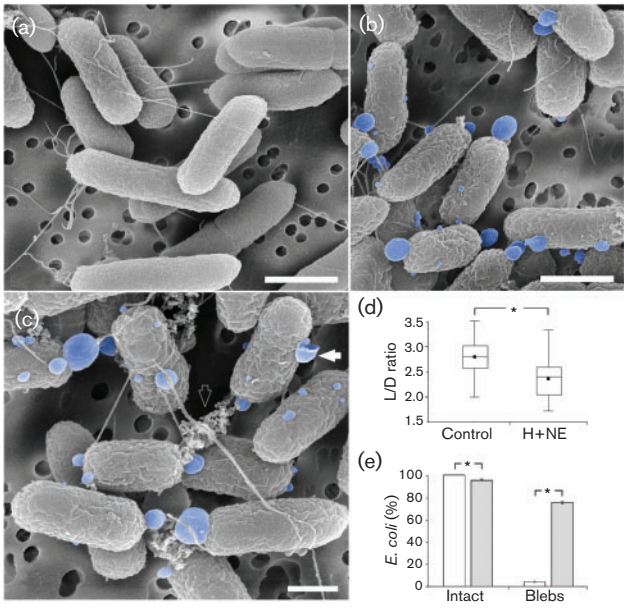

Fig. 4. (a) SEM images of untreated *Escherichia coli* cells. (b) *Escherichia coli* cells subjected to H+NE treatment (1.17 M+6.6 mM). Membrane-bound extracellular attachments are pseudo-coloured in blue. Bars, 1.5 μm. (c) Higher-magnification images further highlighting the cellular debris (open arrow) and the vesicular nature of the surface attachments (white arrow). Bar, 500 nm. (d) Box plots of L/D ratios showing a statistically significant size reduction in the treated cells. (e) Analysis of the proportion of intact versus ruptured cells and quantification of surface blebs in untreated and H+NE-exposed bacteria. White bars, control; grey bars; H+NE. *$P<0.001$. Data are means ± SEM.

2.36±0.13, whereas controls exhibited an L/D ratio of 2.79±0.11 ($P<0.001$) (Fig. 4d).

Dose-dependent and interaction effects

The inhibitory capacity for individual osmotic stress, membrane disruption and hyperosmotic emulsion exposure was determined using turbidity measurements at 24 h. The dose–response curves for each treatment and in concert are shown in Fig. 5(a). For all bacterial strains, the MIC of the membrane-disrupting NEs was determined as 1.65–2.66 mM. *S. aureus* and MRSA were slightly more susceptible, whereas *Escherichia coli* and *Enterococcus faecalis* had approximately the same response. However, the MIC of osmotic stress (2.92 M) for both strains of *S. aureus* was higher than that for *Escherichia coli* and *Enterococcus faecalis* (2.63 M). The dose–response curves for each bacterial strain exposed to H treatment also varied. *Escherichia coli* showed a consistent decrease in population with increasing osmotic pressure. However, at low molar concentrations (<0.29 M), both *Enterococcus faecalis* and *S. aureus* demonstrated a propensity to feed on the saccharides. The slight increase in medium turbidity was most notable with *Enterococcus faecalis*. With higher osmolar solutions, H treatment had a bacteriostatic effect. Plating of the treated bacteria showed that all four strains were capable of surviving in osmotic conditions above 2.92 M (data not shown). In addition, the normalized isobolograms and CI for several specified combinations of H+NE treatment are listed in Fig. 5(b, c). The CI tended to be primarily synergistic (CI <1.0) at most dose combinations, with higher synergy associated with higher H and NE levels. There were a few combinations that were additive, with these mixtures occurring at low sucrose or NE dosages.

DISCUSSION

The biophysical basis for combining membrane disruption with osmotic stress stems from the hypothesis that increased membrane fluidity inhibits osmoregulation and enhances water flux across lipid layers. This concept is an extension of other techniques in which leaky membranes have been exploited to chaperone drugs or dyes into cells (Hancock, 1997; Nikaido, 1994). In the present work, thymol was selected to perturb lipid membranes (Trombetta *et al.*, 2005), whilst sucrose served the role of an osmotic solute. Both of these agents have a history in medicinal use

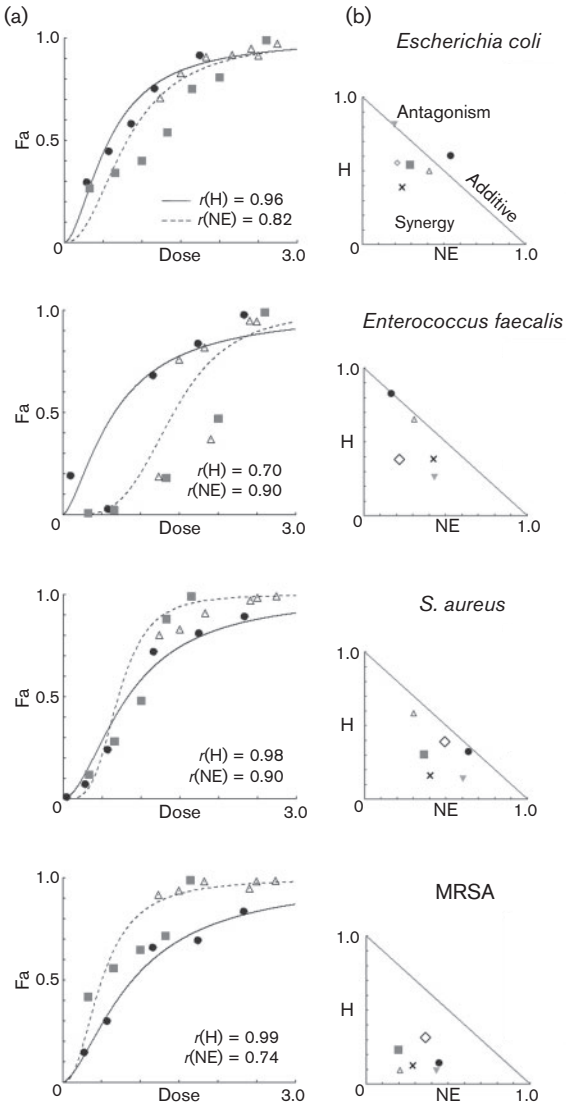

Escherichia coli (MIC_H = 2.63 M; MIC_{NE} = 2.60 mM)

Point	Dose H	Dose NE	Fa	CI
1	0.58	0.66	0.71	1.14
2	1.17	0.66	0.91	0.83
3	1.17	1.00	0.92	0.91
4	1.17	0.33	0.83	1.02
5	1.75	0.66	0.95	0.77
6	1.75	1.00	0.97	0.64

Enterococcus faecalis (MIC_H = 2.63 M; MIC_{NE} = 2.60 mM)

Point	Dose H	Dose NE	Fa	CI
1	0.58	0.66	0.19	2.94
2	1.17	0.33	0.76	1.00
3	1.17	0.66	0.82	0.96
4	1.17	1.33	0.95	0.70
5	1.75	0.66	0.95	0.59
6	1.75	1.33	0.95	0.82

S. aureus (MIC_H = 2.92 M; MIC_{NE} = 1.65 mM)

Point	Dose H	Dose NE	Fa	CI
1	0.58	0.66	0.80	0.96
2	1.17	0.33	0.83	0.89
3	1.17	0.66	0.91	0.89
4	1.17	1.33	0.99	0.74
5	1.75	0.66	0.97	0.67
6	1.75	1.00	0.99	0.57

MRSA (MIC_H = 2.92 M; MIC_{NE} = 1.65 mM)

Point	Dose H	Dose NE	Fa	CI
1	0.58	0.66	0.92	0.59
2	1.17	0.33	0.94	0.43
3	1.17	0.66	0.98	0.31
4	1.17	1.33	0.98	0.52
5	1.75	0.66	0.95	0.67
6	1.75	1.00	0.99	0.41

Fig. 5. (a) Best fit dose–response curves to H and NE exposure for *Escherichia coli*, *Enterococcus faecalis*, *S. aureus* and MRSA. Responses were obtained at 24 h post-treatment. The effect level (Fa) varied between 0 and 1.0, with 0 being no effect and 1.0 being all cells affected. The *r* values for each fitted line, labelled as *r*(H) or *r*(NE), are also given. ●, H (M); ■, NE (mM); △, H+NE. (b) Normalized isobolograms describing the interaction between H and NE. Numbered points correspond to the specific combinations enumerated in the tables in (c). ●, Point 1; ■, point 2; △, point 3; ▼, point 4; ◇, point 5; ×, point 6. (c) Reported MICs and outcomes of six H+NE dose combinations. The units for H and NE were M and mM, respectively. The CI was used to determine the nature of the H+NE interaction. A CI of <1 is defined as synergistic, ~1 is additive and >1 is antagonistic.

with modes of action that are well understood (Boateng *et al.*, 2008; Bowler, 2002; Chirife *et al.*, 1982; Middleton & Seal, 1990). However, there are limited data regarding the combination effects between membrane-acting agents and hyperosmotic challenge. Initial proof of concept of the H+NE combined challenge was first tested on *Escherichia coli*. Cell responses were validated with multiple biomarkers to gain insight into the antibacterial mechanism (Johnston *et al.*, 2003).

Experimental data showed that osmotic stress alone produced negligible changes to cell-membrane permeability and viability. Under osmotic shock, *Escherichia coli* was capable of excluding the membrane probe, whilst corresponding ion-flux measurements demonstrated that cytosolic accumulation of K^+ was used as a means to offset the transmembrane osmotic potential. These results are reflective of prior work, which showed active sequestering of K^+ in the presence of non-ionic hyperosmotic gradients (Wood,

1999, 2011). Additional assessment of cell integrity revealed that osmotic challenge did not induce leakage of intracellular contents. Moreover, short-term ATP levels increased, which is a known adaptation response to hyperosmotic shock (Ohwada & Sagisaka, 1987). Subsequent TEM and SEM imaging indicated signs of cellular dehydration, but there were no indications of plasmolysis or bacteriolysis at 1.17–2.34 M sucrose. These findings are again consistent with previous literature on bacterial osmotolerance (Csonka, 1989; Csonka & Hanson, 1991).

In contrast, *Escherichia coli* subjected to NEs showed increased membrane permeability and irreversible cell damage. For example, PI staining, K^+ flux, intracellular leakage and ATP bioenergetics confirmed that the NEs targeted the cell membrane and induced bacteriolysis. These responses were dose dependent, with the reported MIC comparable to previous values for thymol (Lambert *et al.*, 2001). The TEM images further showed the surfactant-like properties of thymol in which the membrane was denuded or delaminated from the bacterial surface.

Interestingly, the combination of H+NE significantly amplified bactericidal activity versus each agent alone. Membrane staining showed considerable uptake in the vital dye, with results similar to the positive control. K^+ efflux from *Escherichia coli* was observed almost instantaneously, with K^+ leakage approaching 75 % of the total available pool within 30 min. These findings were further corroborated by a significant loss in the amount of leaked nucleic acids. Additionally, cell viability with H+NE decreased by an additional 2 logs when compared with NE alone after 10 min of treatment. These results emphasize that the combination challenge caused highly rapid bacterial inactivation. TEM and SEM imaging indicated a biomechanical phenomenon similar to the additive effects of osmotic stress and membrane damage. Thus, cells exhibited volumetric shrinkage, dehydration, membrane dissolution and bacteriolysis, and whilst most of the cells (>95 %) remained structurally intact, it was evident from the TEM images that there was prominent loss of intracellular material.

The data suggest that the mechanism of action of osmopermeation acts on a timescale of seconds to minutes. This conclusion is not surprising, as strong hyperosmotic environments have been shown to induce cellular shrinkage and plasmolysis in a matter of seconds, whilst surfactants act in a similar time frame (Koch, 1984; McDonnell & Russell, 1999; Russell, 2002). Moreover, whilst the mode of antibacterial activity might be predicted from inspecting the role of the component agents, the overall antibacterial activity was notably enhanced by several orders of magnitude. This striking coupling between hyperosmotic stress and membrane permeability suggests a purely physical phenomenon, whereby the high osmotic pressure instantaneously extracts water and intracellular contents across a compromised membrane (Fig. 6). We emphasize that only cells with damaged membranes were impacted, as healthy cells remained highly viable despite exposure to osmotic

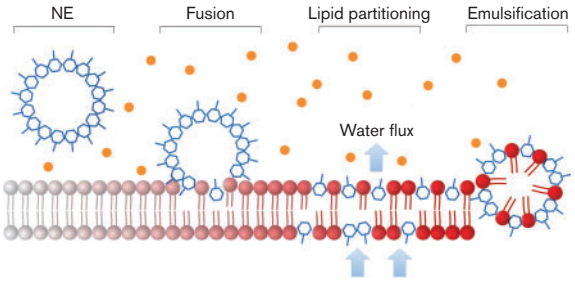

Fig. 6. Proposed mechanism of action for the osmopermeation concept. The fusion of lipophilic NEs induces membrane partitioning and dissolution. Concomitant exposure to a hyperosmotic environment (solute particles in yellow) induces cell shrinkage and bacteriolysis.

pressures of 3–8 MPa. Beyond the initial dehydration, there may be other inhibitory responses resulting in long-term synergism. For example, the reduced cytosolic volume may contribute to viscosity changes that inhibit the vegetative machinery. A hypertonic medium also downregulates DNA replication and upregulates starvation genes. Other adaptations such as the synthesis/importation of compatible solutes are also slower homeostatic responses (Bayles & Wilkinson 2000; Csonka, 1989). Finally, thymol has been shown to have post-application inhibitory effects lasting 12 h or more (Zarrini *et al.*, 2010), whilst phenols are further suspected of causing intracellular coagulation (Russell, 2002).

To assess the wide-spectrum capacity for the H+NE platform, we conducted additional antimicrobial susceptibility studies using other bacterial strains: *S. aureus*, MRSA and *Enterococcus faecalis*. The outcomes of mutual osmotic stress and membrane disruption were analysed using a non-fixed-ratio experimental design and the Chou–Talalay CI (Chou, 2010). The CI is a metric derived from the mass-action law of pharmacokinetics. Possible outcomes in two-drug scenarios include antagonism (CI >1), an additive effect (CI~1) or synergy (CI <1). Dose–response curves showed osmotic stress to be bacteriostatic only at extremely high osmolarities (MIC >2.6 M). Indeed, all strains were capable of surviving in medium with an osmotic pressure of $\geqslant$7.4 MPa after 24 h. This finding is in agreement with previous literature on adaptive osmoregulation (Shabala *et al.*, 2009). For thymol, the MIC for *Escherichia coli* and *Enterococcus faecalis* was 2.66 mM, which is within the range of other *in vitro* studies (Palaniappan & Holley, 2010). The MIC for both *S. aureus* and the MRSA isolate was slightly lower at 1.65 mM. For various combination challenges, we reported a predominant synergy for all bacterial strains. The compound pairings, even at low applied concentrations, suggested that there may be a common synergistic mechanism that is preserved regardless of the cell architecture. Taken together, the CI analysis and companion isobolograms provided dose-oriented *in vitro* combinations needed to achieve a desired effect level.

In our particular experiments, we used a NE (<200 nm in size) to deliver the active membrane-disrupting agent. The advantage of an emulsion is that the force of micelle fusion may additionally damage bacterial surfaces and the tunability of the emulsion lends itself to drug-delivery applications. In the case of thymol, the emulsion platform overcomes the inherent insolubility of the native crystal. However, we believe that the fundamental principle of osmopermeation still applies, regardless of delivery vector or class of surfactant. For instance, quaternary ammonium compounds may be used in place of thymol, whilst polyols or hydrostatic pressure could be substituted for sucrose. To our knowledge, this is the first study to elucidate the synergy between an aqueous membrane-acting compound and hyperosmotic challenge. Previous reports of applying ultrasound and sugar to reduce *Escherichia coli* populations in orange juice have been described (Wong *et al.*, 2008). Yet the specific mechanism by which mechanical energy was coupled to hypertonicity was unclear. These findings may be explained in the context of the current observations, whereby membrane perturbation combined with osmotic gradients enhanced bacteriolysis. We emphasize that the data presented here are applicable to bacteria in the planktonic state and not to adherent cells. Additional work will assess the feasibility of osmopermeation on biofilms and on improving pathogen targeting. The current findings have key implications in disinfectants, antiseptics and wound-dressing formulations for topical treatments.

ACKNOWLEDGEMENTS

This research was funded by the Clinical Translational Science Institute of Indiana Project Development Team pilot grant. The authors would like to acknowledge Michel Schweinsberg for the graphic illustrations and Lynn Guptill for assisting with studies using MRSA and for manuscript proofing.

REFERENCES

Bayles, D. O. & Wilkinson, B. J. (2000). Osmoprotectants and cryoprotectants for *Listeria monocytogenes*. *Lett Appl Microbiol* **30**, 23–27.

Boateng, J. S., Matthews, K. H., Stevens, H. N. & Eccleston, G. M. (2008). Wound healing dressings and drug delivery systems: a review. *J Pharm Sci* **97**, 2892–2923.

Bowler, P. G. (2002). Wound pathophysiology, infection and therapeutic options. *Ann Med* **34**, 419–427.

Brill, J., Hoffmann, T., Bleisteiner, M. & Bremer, E. (2011). Osmotically controlled synthesis of the compatible solute proline is critical for cellular defense of *Bacillus subtilis* against high osmolarity. *J Bacteriol* **193**, 5335–5346.

Carpita, N. C. (1985). Tensile strength of cell walls of living cells. *Plant Physiol* **79**, 485–488.

Chen, C. Z. & Cooper, S. L. (2002). Interactions between dendrimer biocides and bacterial membranes. *Biomaterials* **23**, 3359–3368.

Chirife, J., Scarmato, G. & Herszage, L. (1982). Scientific basis for use of granulated sugar in treatment of infected wounds. *Lancet* **319**, 560–561.

Chou, T. C. (2006). Theoretical basis, experimental design, and computerized simulation of synergism and antagonism in drug combination studies. *Pharmacol Rev* **58**, 621–681.

Chou, T.-C. (2010). Drug combination studies and their synergy quantification using the Chou–Talalay method. *Cancer Res* **70**, 440–446.

Christian, J. H. & Waltho, J. A. (1961). The sodium and potassium content of non-halophilic bacteria in relation to salt tolerance. *J Gen Microbiol* **25**, 97–102.

Codling, C. E., Maillard, J. Y. & Russell, A. D. (2003). Aspects of the antimicrobial mechanisms of action of a polyquaternium and an amidoamine. *J Antimicrob Chemother* **51**, 1153–1158.

Csonka, L. N. (1989). Physiological and genetic responses of bacteria to osmotic stress. *Microbiol Rev* **53**, 121–147.

Csonka, L. N. & Hanson, A. D. (1991). Prokaryotic osmoregulation: genetics and physiology. *Annu Rev Microbiol* **45**, 569–606.

Gould, G. W. (1996). Methods for preservation and extension of shelf life. *Int J Food Microbiol* **33**, 51–64.

Hancock, R. E. W. (1997). The bacterial outer membrane as a drug barrier. *Trends Microbiol* **5**, 37–42.

Hancock, R. E. W. (2007). The end of an era? *Nat Rev Drug Discov* **6**, 28.

Johnston, M. D., Hanlon, G. W., Denyer, S. P. & Lambert, R. J. W. (2003). Membrane damage to bacteria caused by single and combined biocides. *J Appl Microbiol* **94**, 1015–1023.

Koch, A. L. (1984). Shrinkage of growing *Escherichia coli* cells by osmotic challenge. *J Bacteriol* **159**, 919–924.

Lambert, R. J. W., Skandamis, P. N., Coote, P. J. & Nychas, G. J. E. (2001). A study of the minimum inhibitory concentration and mode of action of oregano essential oil, thymol and carvacrol. *J Appl Microbiol* **91**, 453–462.

McDonnell, G. & Russell, A. D. (1999). Antiseptics and disinfectants: activity, action, and resistance. *Clin Microbiol Rev* **12**, 147–179.

Middleton, K. R. & Seal, D. V. (1990). Development of a semisynthetic sugar paste for promoting healing of infected wounds. In *Pathogenesis of Wound and Biomaterial-Associated Infections*, pp. 159–162. Edited by T. Wadström, I. Eliasson, I. Holder & A Ljungh. New York: Springer-Verlag.

Nikaido, H. (1994). Prevention of drug access to bacterial targets: permeability barriers and active efflux. *Science* **264**, 382–388.

O'Byrne, C. P. & Booth, I. R. (2002). Osmoregulation and its importance to food-borne microorganisms. *Int J Food Microbiol* **74**, 203–216.

Ohwada, T. & Sagisaka, S. (1987). An immediate and steep increase in ATP concentration in response to reduced turgor pressure in *Escherichia coli* B. *Arch Biochem Biophys* **259**, 157–163.

Palaniappan, K. & Holley, R. A. (2010). Use of natural antimicrobials to increase antibiotic susceptibility of drug resistant bacteria. *Int J Food Microbiol* **140**, 164–168.

Pilizota, T. & Shaevitz, J. W. (2012). Fast, multiphase volume adaptation to hyperosmotic shock by *Escherichia coli*. *PLoS ONE* **7**, e35205.

Russell, A. D. (2002). Mechanisms of antimicrobial action of antiseptics and disinfectants: an increasingly important area of investigation. *J Antimicrob Chemother* **49**, 597–599.

Shabala, L., Bowman, J., Brown, J., Ross, T., McMeekin, T. & Shabala, S. (2009). Ion transport and osmotic adjustment in *Escherichia coli* in response to ionic and non-ionic osmotica. *Environ Microbiol* **11**, 137–148.

Trombetta, D., Castelli, F., Sarpietro, M. G., Venuti, V., Cristani, M., Daniele, C., Saija, A., Mazzanti, G. & Bisignano, G. (2005). Mechanisms of antibacterial action of three monoterpenes. *Antimicrob Agents Chemother* **49**, 2474–2478.

Walsh, S. E., Maillard, J. Y., Russell, A. D., Catrenich, C. E., Charbonneau, D. L. & Bartolo, R. G. (2003). Activity and mechanisms of action of selected biocidal agents on Gram-positive and -negative bacteria. *J Appl Microbiol* **94**, 240–247.

Wong, E., Pérez, A. M. & Vaillant, F. (2008). Combined effect of osmotic pressure and sonication on the reduction of *Salmonella* spp. in concentrated orange juice. *J Food Saf* **28**, 499–513.

Wood, J. M. (1999). Osmosensing by bacteria: signals and membrane-based sensors. *Microbiol Mol Biol Rev* **63**, 230–262.

Wood, J. M. (2011). Bacterial osmoregulation: a paradigm for the study of cellular homeostasis. *Annu Rev Microbiol* **65**, 215–238.

Zarrini, G., Delgosha, Z. B., Moghaddam, K. M. & Shahverdi, A. R. (2010). Post-antibacterial effect of thymol. *Pharm Biol* **48**, 633–636.